nature astronomy

Article

https://doi.org/10.1038/s41550-022-01802-z

Acquisition and Preservation of Remanent Magnetization in Carbonaceous Asteroids

Received: 22 December 2021

Accepted: 6 September 2022

Published online: 13 October 2022

Check for updates

Samuel W. Courville[1], Joseph G. O'Rourke[1], Julie C. Castillo-Rogez[2], Roger R. Fu[3], Rona Oran[4], Benjamin P. Weiss[4] and Linda T. Elkins-Tanton[1]

The solar nebula sustained a strong magnetic field that may have aided planetesimal accretion and imparted the chemical remanent magnetization (CRM) observed in some carbonaceous chondrite meteorites. The CRM thus provides a record of the magnetic field of the early Solar System at the time when carbonaceous chondrite parent bodies experienced aqueous alteration. However, the link between CRM recorded in carbonaceous chondrites and the geophysical evolution of carbonaceous chondrite parent bodies has not been thoroughly investigated. Using planetesimal thermal evolution models, we show that CRM in carbonaceous chondrites would be a natural consequence of water-rich planetesimals forming within the solar nebular magnetic field. We find that large carbonaceous chondrite parent bodies (>50 km radius), which never hosted endogenous dynamo-driven magnetic fields due to their lack of metallic cores, could have strong, present-day remanent magnetism from the ancient nebular magnetic field. In situ magnetometer measurements of large C-type asteroids could therefore validate models of carbonaceous chondrite magnetization by the solar nebular magnetic field. We suggest that 2 Pallas may be a good target for such a study.

Several meteorites in two groups of carbonaceous chondrites, the CM and CV chondrites, host a chemical remanent magnetization (CRM)[1,2] and possibly also thermoremanent magnetization[3]. CRM in a meteorite implies that chemical reactions produced ferromagnetic minerals within the meteorite's parent body while in the presence of a strong and temporally stable magnetic field. CM and, to a limited extent, some CV chondrites experienced aqueous alteration[4,5]. Aqueous alteration can produce minerals that are potential magnetic carriers[4], such as magnetite (Fe_3O_4) and pyrrhotite ($Fe_{(1-x)}S$, $x = 0$–0.2). Ferromagnetic minerals that form in the presence of a background magnetic field can acquire a CRM in the same direction as the background field[6–8]. Thus, CRM in CM and CV chondrites probably indicates that their parent bodies underwent aqueous alteration in the presence of a strong magnetic field.

The magnetic field sustained by the cloud of dust and gas in the early solar nebula is likely to be the source of some of the magnetization in CM chondrites[1] and CV chondrites[2]. Pre-accretional thermal remanent magnetization within chondrules of primitive LL and CO chondrites indicates that the early solar nebula probably had a strong magnetic field that was active in the first few million years (Myr) of the Solar System's history[2,9,10]. It is likely that the nebula supported a strong magnetic field until at most ~3.9 Myr after the formation of calcium aluminium inclusions (CAIs) in the inner Solar System, or at most ~4.8 Myr in the outer Solar System[9]. We use thermal evolution models to determine whether planetesimals could experience aqueous alteration before the nebula dissipated—and thus whether asteroids, today, could retain chemical remanence from the nebular field like the CRM that is found in CM and CV chondrites.

[1]School of Earth and Space Exploration, Arizona State University, Tempe, AZ, USA. [2]Jet Propulsion Laboratory, California Institute of Technology, Pasadena, CA, USA. [3]Department of Earth and Planetary Sciences, Harvard University, Cambridge, MA, USA. [4]Department of Earth, Atmospheric and Planetary Sciences, MIT, Cambridge, MA, USA. e-mail: swcourvi@asu.edu

https://doi.org/10.1038/s41550-022-01802-z

Results

Thermal evolution modelling

During the heating of a planetesimal's interior through the radioactive decay of ^{26}Al, two important thermal events determine the potential for acquiring a chemical remanent magnetization. First, the planetesimal reaches the melting point of water ice (~273 K). When water ice melts, the resulting liquid water chemically reacts with rock and produces the magnetic carriers magnetite and pyrrhotite[4]. If these minerals formed before the dissipation of the solar nebula, the nebular field would impart a CRM on the minerals. The second event occurs if the planetesimal reaches a high enough temperature to erase or overprint CRM. The Curie temperature for a mineral is the temperature above which the mineral would completely lose ferromagnetic behaviour. Heating a mineral above its Curie temperature in the absence of a magnetic field erases the mineral's magnetization. Individual mineral grains may also unblock (demagnetize) at temperatures slightly below the Curie point. The precise unblocking temperature for each individual grain depends on a priori unknowns such as its size, shape and the duration it is exposed to elevated temperatures[11], although unblocking temperatures of grains just below the Curie temperature are relatively insensitive to heating duration[12]. Consequently, we adopted single fixed unblocking temperatures that are within empirically measured ranges relevant to the bulk behaviour of magnetized CM chondrites[1]: 550 K for pyrrhotite and 850 K for magnetite (versus Curie temperatures of 583 K and 858 K, respectively). These temperatures offer a cautious representation of thermal demagnetization, allowing nebular magnetization to be overprinted under a slightly larger range of metamorphic scenarios than if we assumed demagnetization at the Curie temperature. If the planetesimal heats to the unblocking temperature(s) of its magnetic carrier(s) after the nebular magnetic field dissipates, then any CRM from the nebular field would be lost. Lastly, if portions of a planetesimal were to heat above, but then cool below, the Curie temperature(s) before the end of the lifetime of the nebula, then they would acquire a thermoremanence.

We calculated the temperature inside a planetesimal as it heats over time through radioactive decay (see Methods for thermal modelling details and assumptions). Depending on the timing of aqueous alteration and magnetic unblocking with respect to the lifetime of the solar nebular magnetic field, our planetesimal models fell into one of three thermal evolution cases. In the first case, a planetesimal may form too late to reach the temperature to melt water ice before the solar nebula dissipates (Fig. 1a). This case results in no nebular magnetization and may be relevant to unmagnetized carbonaceous chondrites like CRs[9]. In the second case, a planetesimal may form early enough to melt water ice and undergo aqueous alteration before the nebula dissipates but not subsequently heat beyond the unblocking temperatures of magnetite or pyrrhotite (Fig. 1b). This scenario could lead to magnetization of nearly the entire planetesimal. In the third case, a planetesimal could form early enough to undergo aqueous alteration, but subsequently heat beyond the unblocking temperatures (Fig. 1c). Our models indicate that an undisturbed planetesimal (that is, one that did not experience impact unroofing and rapid cooling[13]) that heats beyond the unblocking temperature does not cool below that threshold again until after the nebula dissipates and therefore could not retain CRM or acquire thermoremanent magnetization in its interior that is a record of the nebular field. However, a shell of aqueously altered chondritic material a few kilometres thick that does not reach the unblocking temperature could retain magnetization near the surface. Thus, magnetized CM or CV chondrites could originate from either the second or third case. Only the second case produces asteroids with large-scale remanent magnetization from the solar nebula.

Figure 2 plots the maximum volume percentage of a planetesimal that the solar nebular magnetic field could magnetize as a function of the planetesimal's radius and formation time. For a planetesimal to acquire large-scale magnetization within both pyrrhotite and magnetite, the planetesimal must form between ~3.5 and 3.7 Myr after CAIs (Fig. 2a), assuming the nebular field dissipates 4.8 Myr after CAIs, which is the upper-bound dissipation time for the outer Solar System where carbonaceous chondrites formed[9] (Extended Data Fig. 1 explores a quicker nebula dissipation time). As magnetite has a higher unblocking temperature, earlier-forming and therefore hotter planetesimals could retain magnetization solely within magnetite. For magnetite, large-scale magnetization is possible for planetesimals that form between ~2.7 and 3.7 Myr after CAIs (Fig. 2b). These ranges are consistent with the formation time estimated for the parent bodies of the CM and CV chondrites[14–18]. Our thermal models assumed that each planetesimal accretes instantly with 40 vol% water ice, which is consistent with the ~20–40% range interpreted for the parent body/bodies of the CM chondrites[19,20]. Raising the amount of water ice reduces heating, which allows earlier formation times and therefore broadens the range of time that would allow magnetization. The parent body/bodies of the CV chondrites probably accreted with <12.5 vol% water[20], which would cause more heating and reduce the range of times that would allow magnetization (Extended Data Fig. 2).

Aqueous alteration and scale of uniform magnetization

Large-scale remanent magnetization within a planetesimal may or may not produce a strong magnetic field. The strength of the magnetic field depends greatly on how much of the body is uniformly magnetized—that is, how much volume within the planetesimal acquires magnetization in the same direction. For a portion of a planetesimal to be uniformly magnetized, it must experience aqueous alteration over a period that the nebular field maintains a constant direction. To experience simultaneous alteration, a volume must be exposed to fluid at the same time. Our thermal models assume that liquid water separates from rock after the ice melts (that is, water flows through rock on its way to the surface). We argue that uniform magnetization would occur over the distance that water can travel during the period that the nebular field is stable. Under this argument, the faster the fluid flow, the larger the length scale of magnetization.

We assumed an exhalation alteration model; that is, single-pass fluid flow directed to the surface[21] where pressure forces the mobile and less dense water to the surface[22]. Under this assumption, the effective permeability of the planetesimal determines how quickly the water reaches the surface. We adopted this hypothesis because it is consistent with our thermal evolution modelling and enabled quantitative predictions for the length scale of CRM in planetesimals, although we discuss how other aqueous alteration models yield similar predictions in subsequent paragraphs. If the distance over which fluid flows during the time that the solar nebular field is coherent determines the length scale, then the effective permeability of the planetesimal is the critical parameter. Our thermal models assumed that the flow of water to the surface is much faster than the thermal evolution: all water flows to the surface within 250 kyr, implying a permeability of at least ~10^{-14} m^2 (see methods). Assuming a nebular field stability time of 1 kyr (ref. [9]), and an effective permeability between 10^{-13} and 10^{-12} m^2, which is applicable for a fractured chondritic body[23], Fig. 3 demonstrates that magnetization length scales would be ~10–100 km (Extended Data Fig. 3 explores an unrestricted parameter space with similar results). Exhalation alteration on a body that accreted with a large volume of water ice could therefore yield an asteroid with large-scale uniform magnetization within magnetic mineralogy similar to that observed in the CM chondrites.

Exhalation alteration successfully predicts water–rock differentiation in bodies and the existence of altered chondrites. However, not all chemical details of the CM chondrites match with the exhalation flow model. The mineralogy of CM chondrites suggests that alteration was isochemical, possibly meaning that during alteration, the water was stagnant and did not flow through material[24]. This could be the case if the planetesimal was originally extremely impermeable:

 https://doi.org/10.1038/s41550-022-01802-z

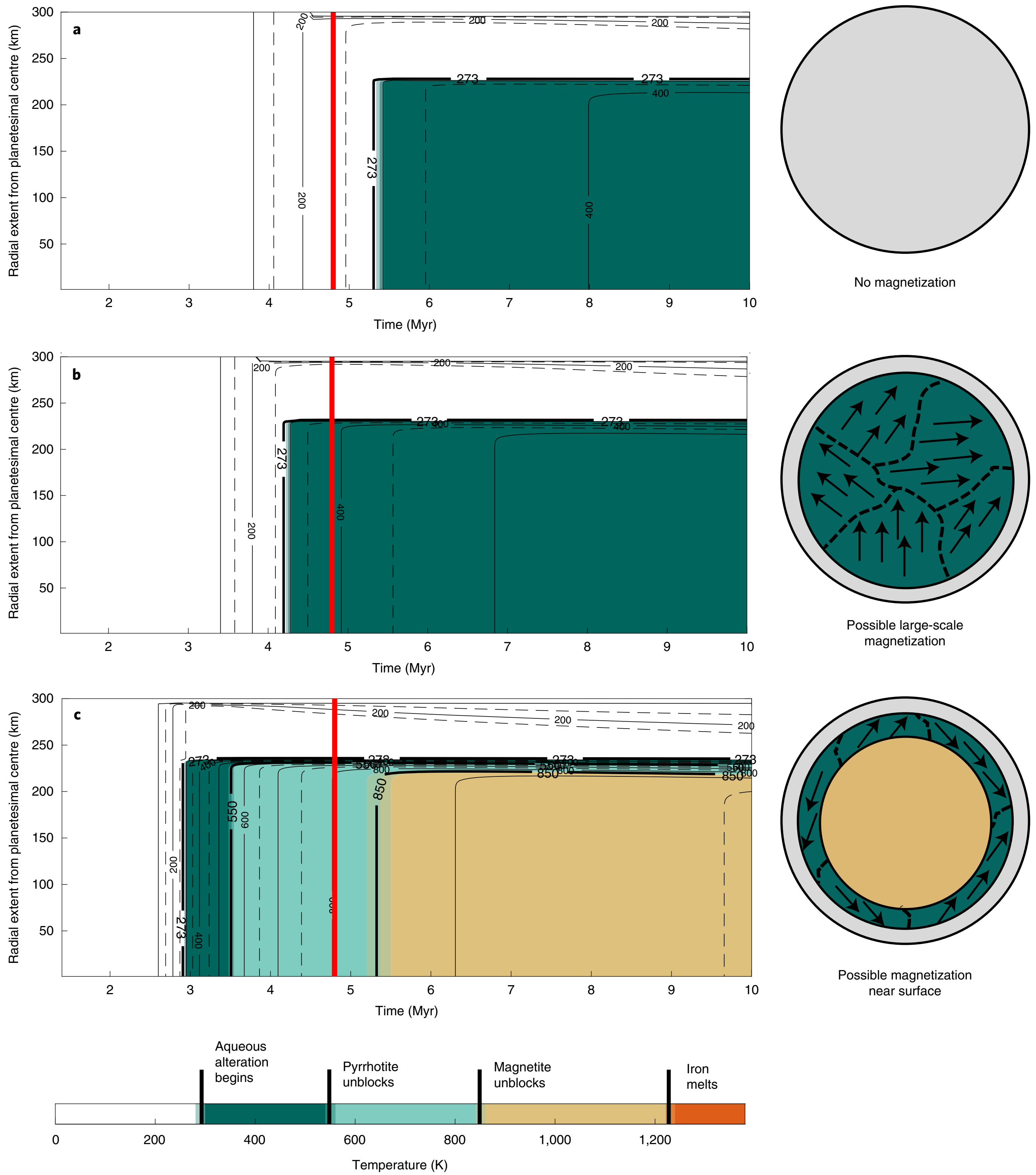

Fig. 1 | Planetesimal thermal evolution determines the extent of aqueous alteration and thus the magnetizable volume. a–**c**, Thermal evolution models for a 300-km-radius spherical planetesimal accreted with 40 vol% ice at 3.8 Myr (**a**), 3.4 Myr (**b**) and 2.6 Myr (**c**) after CAIs. The contours represent the temperature (K) inside the planetesimal as a function of the position within the planetesimal and the time after CAIs (thin solid and dashed contours are at intervals of 100 K and 50 K, respectively). **a**, The planetesimal forms too late for ^{26}Al-driven heating to trigger aqueous alteration (~273 K) before the solar nebular field dissipates (red vertical bar). This case leads to no magnetization. **b**, The planetesimal forms early enough for aqueous alteration to occur and does not subsequently exceed the unblocking temperatures of the magnetic minerals (~550 K for pyrrhotite, ~850 K for magnetite). This scenario permits possible magnetization throughout the entire body. **c**, The planetesimal heats enough to experience aqueous alteration before the nebular field dissipates, but subsequently exceeds the unblocking temperatures for most of the interior. This evolution means that the majority of the planetesimal would be demagnetized except for a shell near the surface. The corresponding interpretive diagrams (right) indicate regions of plausible magnetization with arbitrarily oriented vector arrows. None of the scenarios reach a high enough temperature to melt iron (1,261 K at the iron–sulfur eutectic point[79]), as indicated by the lack of orange in the plots.

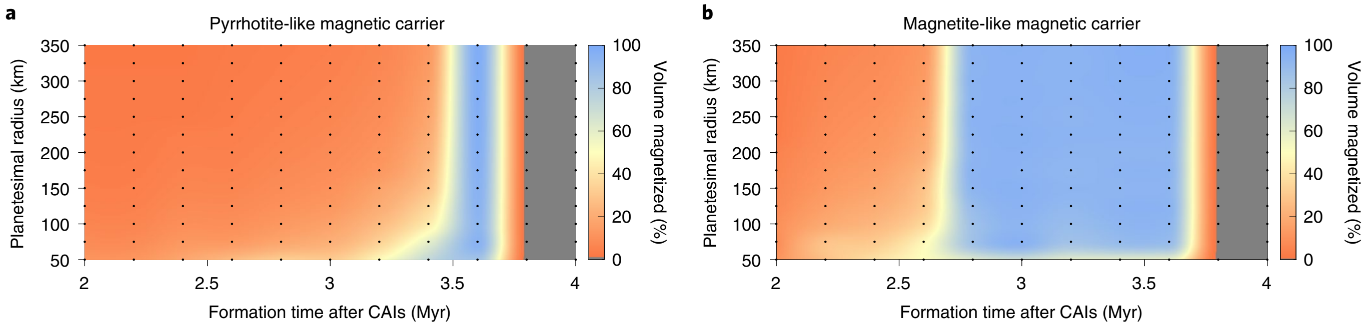

Fig. 2 | Formation time determines the maximum possible magnetized rock volume and magnetic moment that a planetesimal could acquire. a,**b**, The maximum possible volume of the planetesimal that the solar nebular field could magnetize as a function of the planetesimal's formation time and radius with pyrrhotite (**a**) and magnetite (**b**) as the magnetic carriers. A wide range of formation times leads to ~100% magnetization if the magnetic carrier is magnetite. If the magnetic carrier is pyrrhotite, then the extent of magnetization is more sensitive to formation time. Grey regions indicate negligible magnetized volume. Black dots represent individual thermal model runs. The plots assume planetesimals with 40 vol% water ice that the solar nebular field dissipated 4.8 Myr after CAIs with unblocking temperatures of 550 K for pyrrhotite and 850 K for magnetite.

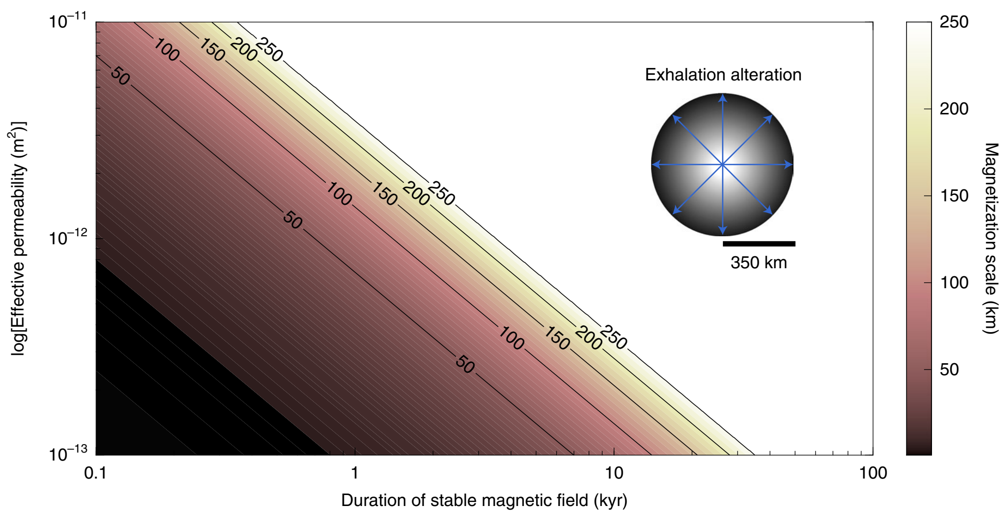

Fig. 3 | A permeable planetesimal could have large-scale uniform magnetization. The scale of uniform magnetization within a permeable planetesimal with a 350 km radius as a function of the planetesimals' effective permeability and the period that the nebular magnetic field has a stable direction. This plot assumes exhalation alteration, where pressure forces water outwards from the planetesimal's interior. The more permeable the planetesimal, or the greater the stability time of the nebular field, the greater the magnetization length scale. Extended Data Fig. 3 displays a full set of relationships between magnetization scale and the other thermal evolution and alteration parameters.

10^{-19}–10^{-17} m^2. In this case, the length scale of uniform magnetization would not be dependent on fluid flow—it would instead depend on how homogeneous the planetesimal's starting composition was. If ice and rock were homogeneously distributed throughout the body, and the body heated homogeneously, then large-scale uniform magnetization would result. The length scale of magnetization would thus represent the scale of heterogeneous distributions of water ice, which would cause heterogeneity in the amount of radiogenic heating from the silicate component. In the absence of heterogeneity constraints, this model can lead to any magnetization length scale value. The alteration environment may last well beyond the lifetime of the solar nebula. Regardless, any magnetic minerals that form before the nebular field dissipates will acquire magnetization. So long as subsequent alteration does not alter the magnetized mineral phases, the magnetization will remain throughout the duration of alteration.

Debates over permeability and whether alteration was isochemical can be bypassed altogether if aqueous alteration occurred in unlithified rock. In this scenario, water melting leads to a muddy mixture of mobile pebbles[25]. As both the pebbles and the fluid are well mixed and mobile, a muddy planetesimal may experience 'mudball' convection, wherein both solids and fluid move about the asteroid to dissipate heating[25,26]. This model would match geochemical studies of CM chondrites that indicate alteration occurred isochemically[24,27]. The whole-body convection could extend from the mud-mantle to the core. The sorting of particle sizes and variable water-to-rock ratios throughout a convecting mudball would lead to compositional heterogeneity throughout the body[25] because reactions with differing water-to-rock ratios would produce differing secondary minerals. We expect that magnetization length scales would be on the order of ~10–100 km on the basis of the size of convective cells in modelling studies[25]. However, to accurately estimate the length scale of uniform magnetization in a convecting mudball, one must carefully consider the chemical evolution and orientation of solids. An extension of the mudball model of this magnitude is outside the scope of this Article but may be warranted in the future if the mudball model emerges as the dominant mode of alteration in the Solar System.

CV chondrites[28], and some CM chondrites that experienced dehydration[29–32], may have been exposed to higher temperatures. High-temperature hydrothermal systems may occur within planetesimals[33]. Indeed, hydrothermal reactions in fumarolic-like systems

https://doi.org/10.1038/s41550-022-01802-z

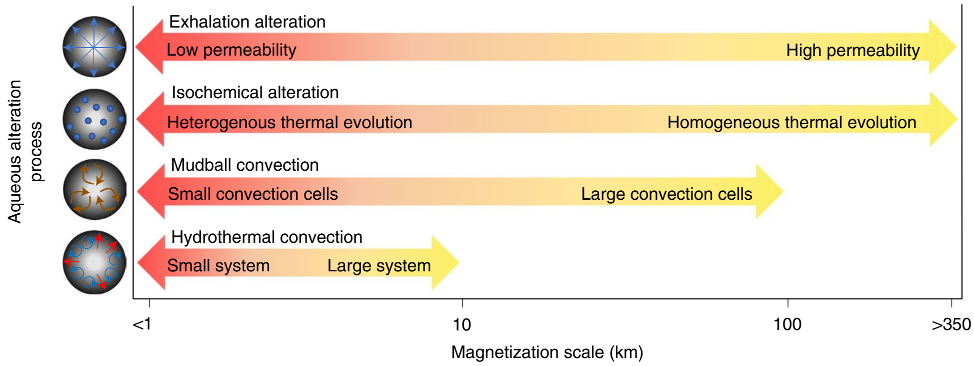

Fig. 4 | Different aqueous alteration models result in different ranges in the possible length scale of uniform remanent magnetization. The prevailing aqueous alteration process changes the maximum possible uniform magnetization scale, which is the effective radius of the volume that is uniformly magnetized. For exhalation flow, effective permeability controls the magnetization length scale. In the corresponding conceptual diagram at left, the blue arrows signify fluid flow outward from the planetesimal's center. In an isochemical model, the magnetization scale would depend on the homogeneity of the ice/rock ratio that controls thermal evolution. At left, the blue dots signify stagnant water within the planetesimal. In a mudball, the size of convective cells controls the maximum length scale. At left, the brown circular arrows signify large convection cells of water mixed with solids. For hydrothermal convection, high-temperature fumarolic alteration would only operate near the planetesimal surface, <10 km, where steep thermal gradients exist, and the magnetization scale would depend on the size of the hydrothermal system. At left, the red arrows symbolize the steep thermal gradient that leads to near surface fluid convection represented by the blue circular arrows.

that involve effusive steam events are potentially able to alter minerals much more quickly (tens of years or less) than conventional fluid alteration[34]. If alteration occurs as the result of effusive events where high-temperature fluid and steam escape the subsurface, then alteration would probably occur in distinct separate events and perhaps be similar to hydrothermal alteration environments in terrestrial ocean spreading centres[35]. From analogous terrestrial hydrothermal systems[36], we expect that the magnetization length scale of such a system could be on the order of ~1–10 km, depending on the size of the system. If aqueous alteration occurs over multiple-pass hydrothermal pore-fluid convection, then the length and timescales of convection could determine the magnetization length scale. Pore-fluid and/or hydrothermal convection could have length scales of ~10 km but require a steep thermal gradient, which would only exist near the surface[27,37]. Unlike the previous alteration scenarios, this scenario is consistent with a hotter planetesimal thermal evolution. For example, in the case from Fig. 1c, the temperature may exceed the Curie point of pyrrhotite—and thus only magnetite could retain magnetization.

In summary, different models of aqueous alteration predict various upper bounds for the length scales of magnetization (Fig. 4). Assuming a permeable planetesimal that undergoes exhalation alteration, we expect magnetization scales to be ~10–100 km. For an impermeable planetesimal, alteration scales could range widely depending on the homogeneity of thermal evolution throughout the body (for example, from <1 km to >100 km). For whole-body mudball convection[25], the length scale could be as great as 100 km if alteration occurs homogeneously throughout convective cells within the mudball. Under the realm of hydrothermal fluid convection, we expect that only the near surface within ~10 km of the surface would have the temperature gradient necessary to sustain convection, so length scales would be ~10 km. If fumarolic systems dominate magnetization, then (based on terrestrial hydrothermal scale) the length scale could be on the order of 1–10 km. It is possible that each of these alteration modes may have occurred somewhere in the Solar System, or even within the same body. Improved models would help us refine predictions for meteoritic analyses and spacecraft observations, which are the ultimate tests of all models for the aqueous alteration of planetesimals.

Regardless of the magnetization length scale that a planetesimal acquires, the potential present-day length scale of magnetization in a C-type asteroid would depend on whether it survived disruption from impacts. If an asteroid was catastrophically disrupted into a rubble pile, then the largest scale of magnetization possible would be the size of its largest rubble pieces. Large asteroids, such as 2 Pallas, are probably intact[38], although they have certainly been battered by impacts and could have lost a substantial amount of water[39]. Large impacts would disrupt magnetization near the surface as they excavate and scramble material from several kilometres beneath the subsurface. For example, the largest known basin on 4 Vesta, Rheasilvia basin, excavated material from ~40 km deep[40]. The lunar megaregolith is probably ~20 km thick[41]. Therefore, any large-scale magnetization near the surface is unlikely to be retained, but magnetization kilometres beneath the surface of an intact asteroid could survive.

Magnetic field detectability

If the solar nebular field magnetized large C-type asteroids uniformly on a large scale, then a spacecraft may be able to detect remanent fields that have persisted until today. To assess detectability, we estimated the magnetopause altitude for a spherical asteroid with a radius of 250 km orbiting at 2.8 au in the present-day solar wind. The magnetopause altitude is determined by the balance between the magnetic pressure of the body countering the gas flow pressure of the solar wind (Methods). Figure 5 plots the magnetopause altitude as a function of the length scale of magnetization within the asteroid. We accounted for the likely effects of impacts scrambling the near surface by assuming that uniform magnetization may not be present until 20 km into the subsurface. The higher the magnetopause, the more easily detectable the asteroid's magnetic field would be. Assuming a magnetization intensity of 10^{-4} A m^2 kg^{-1}, the average value measured in CM chondrites[1], we found that a magnetization length scale of at least ~20 km would result in a magnetopause altitude sufficient for a spacecraft magnetometer to fly through.

The exact minimum altitude at which a spacecraft could detect a magnetic field of a given strength depends on the specific mission design, and the orientation and interaction of the magnetized regions with the solar wind. Moreover, while the detection of a magnetic field would validate the hypothesis that large-scale uniform magnetization is present, the absence of a magnetic field detection would not rule out the presence of materials magnetized in the solar nebula because short length-scale magnetization producing field strengths below the detection limit could still exist. Surface magnetic field measurements could probably detect shorter uniform magnetization length scales.

https://doi.org/10.1038/s41550-022-01802-z

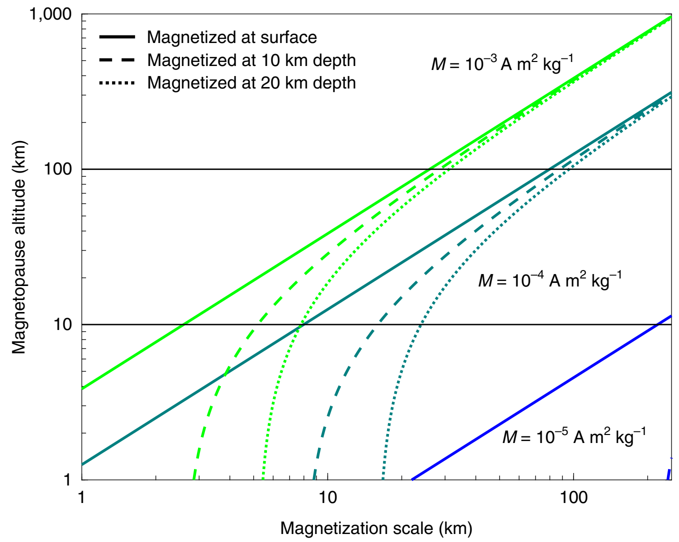

Fig. 5 | A chondritic asteroid with large-scale magnetization can produce a magnetopause above the asteroid's surface that could be detectable by spacecraft. Assuming a 250-km-radius asteroid, about the size of 2 Pallas, the curves represent the altitude of the magnetopause as a function of the magnetization scale for magnetization intensities, M, of 10^{-3}, 10^{-4} and 10^{-5} A m^2 km^{-1} (light green, dark green, and blue, respectively). The dashed and dotted curves represent how the magnetopause altitude is reduced if there are 10 and 20 km layers, respectively, of unmagnetized material atop the magnetized material, which accounts for near-surface magnetization being erased or scrambled by impacts. At short magnetization scales, the magnetopause distance depends greatly on the depth to magnetization, with deeper magnetization being more difficult to detect.

Discussion

Given our findings, we consider the asteroid 2 Pallas as a potential target. 2 Pallas is a candidate parent body for the CM chondrites[38] because it exhibits a hydrated spectral signature in the 3 μm region, which matches CM chondrite spectra[42]. Impacts can produce the observed differences between the visible and near-infrared spectra of Pallas and the CM chondrites[38]. Furthermore, the bulk density of Pallas (~2.9 g cm^{-3}) is similar to the grain density of CM chondrites[43]. Pallas also seems to lack a thick icy shell, based on its global morphology[38], unlike Ceres[44]. A possible model for Pallas' evolution is that it underwent aqueous alteration on a global scale and subsequently lost the remaining water ice as a consequence of subcatastrophic impacts, as suggested by the large basins found on its surface[38,39]. An early phase of hydrothermal evolution could also limit heating and separation of a metallic core[38]. Our thermal models show that if Pallas formed between 2.7 and 3.5 Myr after CAIs, then Pallas could retain large-scale magnetization from the nebular field.

Overall, our work describes how a planetesimal that formed a few million years after CAIs would undergo enough heating to acquire a CRM during aqueous alteration while embedded within the solar nebular field, but not enough heating to later erase the CRM. We predict that large C-type asteroids could have magnetospheres detectable from spacecraft. We hypothesize that 2 Pallas could be one such asteroid and suggest that this hypothesis be tested with low-altitude, spacecraft magnetic field measurements. Detecting a magnetic field around a C-type asteroid would illuminate the extent of its internal aqueous evolution and whether it formed in the presence of the solar nebular magnetic field.

Methods

Thermal evolution models

Thermal evolution controls how and when a planetesimal may acquire CRM through aqueous alteration. We employed the thermal modelling algorithm described by Castillo-Rogez and colleagues[45–47]. This algorithm solves for the temperature profile at each radial extent:

$$\frac{\mathrm{d}\left(\frac{\kappa(T)\mathrm{d}T(r)}{\mathrm{d}r}\right)}{\mathrm{d}r} + \frac{2}{r}\left(\frac{\kappa(T)\,\mathrm{d}T(r)}{\mathrm{d}r}\right) = \rho(r)\,C_p(T)\left(\frac{\mathrm{d}T(r)}{\mathrm{d}t}\right) - H(r),$$

where T is the temperature (K), r is the radius (m), κ is the thermal conductivity (W m^{-1} K^{-1}), ρ is the density (kg m^{-3}), C_p is the specific heat capacity (J K^{-1} kg^{-1}) and H is the specific heat production from radiogenic decay (W kg^{-1}). We take the initial ^{26}Al concentration as 650 parts per billion for a mean chondritic composition and 0.355 W kg^{-1} for its specific heat production[47]. The model assumes a mixed composition of water ice and silicates, which have heat capacities of $(185 + 7.037T)$ J K^{-1} kg^{-1} and 920 J K^{-1} kg^{-1}, respectively, and thermal conductivities of $(0.4685 + 488.12/T)$ W m^{-1} K^{-1} and 4.2 W m^{-1} K^{-1}, respectively. The model time step is 10^4 yr. This thermal model also includes heating from accretion:

$$T(r) = \frac{h}{C_p(T)}\left[\frac{4\pi}{3}\rho\, G\, r^2 + \frac{\upsilon^2}{2}\right] + T_i,$$

where h is the fraction of mechanical energy transferred to heat (unitless), G is the gravitational constant (N m^2 kg^{-2}), υ is the velocity of accreting objects (m s^{-1}), and T_{i} is the initial temperature (K). Even for the largest planetesimals we considered, the heat from accretion[48] is only a few tens of kelvin, so the assumption of instantaneous accretion is acceptable.

We modelled an array of planetesimals with varying radii and formation time. Radii range from 50–350 km in increments of 25 km and formation times range from 2–4 Myr after CAIs in increments of 0.2 Myr. Additionally, we run each model with a starting water ice volume fractions of 10 and 40%. We also run each model with initial temperatures of 100 and 160 K, which correspond to possible outer (between the orbits of Jupiter and Uranus) and inner solar nebula temperatures, respectively (for example, Boss 1993)[49], noting that many possible solar nebula temperature profiles have been proposed in the literature.

Magnetic field calculation

The magnetic dipole moment is defined as:

$$m = \iiint \rho\, \mathbf{M}\, \mathrm{d}V,$$

where $\mathbf{M}$ is the mass magnetization (A m^2 kg^{-1}) and V is the magnetized volume (m^3). In general, an asteroid can be non-spherical, and the volume can be composed of fractions that have varying magnetization strengths and directions. To calculate the dipole moment from a magnetized volume, we assumed that the entire volume had the same magnetization direction and magnetization intensity. The dipole moment m (A m^2) then simplifies to the product of the magnetization magnitude, density and the magnetized volume:

$$m = \rho M V.$$

The true magnetization value that can be achieved within a planetesimal depends on many factors: the strength and orientation of the nebular field relative to the planetesimals rotation axis, the abundance of secondary magnetic minerals and the efficiency with which they acquire magnetization. However, these parameters are not well enough constrained to provide a precise estimate of magnetization[50,51]. We therefore assumed that the magnetization value of CM chondrites is representative of the magnetization value that could be acquired during aqueous alteration of a planetesimal. We assumed a nominal magnetization value of 10^{-4} A m^2 kg^{-1}, which is about the average magnetization value measured in CM chondrites[1]. This value is indicative of the magnetization component attributed to natural post-accretional, asteroidal remanent magnetization, as opposed to magnetization acquired subsequently by magnetic contamination on Earth. However, in Fig. 5 we also consider higher and lower values, 10^{-3} A m^2 kg^{-1} and 10^{-5} A m^2 kg^{-1}, to illustrate the effect of higher or lower magnetization.

The output of a planetesimal thermal model tells us what volume of the planetesimal can be magnetized. However, it is idealistic to assume that the solar nebula would magnetize an entire asteroid unidirectionally. A certain volume portion of a planetesimal would only acquire uniform magnetization if it experienced aqueous alteration during a period where the solar nebular magnetic field had a constant direction. However, a rotating planetesimal orbiting around the early Sun would have had an ever-changing orientation with respect to the nebular field. In this case, the planetesimal would acquire remanent magnetization in the net average direction of the background field parallel to the planetesimal's spin axis[52]. The intensity and direction of the solar nebular field was probably stable for periods of ~1 kyr or longer[9]—long enough to allow magnetic minerals to form during a planetesimal's aqueous alteration[8]. If the planetesimal's spin axis was not perfectly aligned with the disk plane, the projection of the spin axis onto the vertical component of the nebular field in the protoplanetary disk would have a non-zero average, as the vertical component would remain constant as the planetesimal orbits around the Sun, thus allowing magnetization in that direction.

If fluid flow from the core to the surface of a planetesimal drives the rate at which aqueous alteration occurs, the permeability of the planetesimal determines the length scale of magnetization. Under the assumption of Darcy fluid flow, the pressure (P) gradient in the body drives fluid to the surface[22]. The pressure gradient at a depth z (m) is defined as:

$$\frac{\mathrm{d}P}{\mathrm{d}z} = \rho g(z)$$

where and g is gravitational acceleration (m s^{-2}). The linear fluid velocity (m s^{-1}) in a porous medium governed by Darcy's law follows the relationship:

$$v(z) = \frac{k}{\mu\phi}\frac{\mathrm{d}P}{\mathrm{d}z}$$

where k is permeability (m^2), μ is fluid viscosity (Pa s) and ϕ is porosity (unitless). Dividing the expected stability time of the nebular field by v yields an estimate of the magnetization length scale. We report the length scale using the maximum fluid flow velocity within the body. The fluid viscosity of water is 10^{-3} Pa s.

We assumed that the length scale corresponds to the radius of a spherical volume, and that the effective dipole moment is given by the product of the spherical volume and the magnetization value. At a spacecraft flyby distance (that is, closest approach of 10–100 km from the surface of the planetesimal, depending on the mission design), a collection of randomly oriented magnetized regions of similar size would produce a field strength that is approximately the same as the field strength that would come from the dipole moment of just one of the magnetized regions[53].

Magnetopause distance

To assess the detectability of a magnetized Pallas, we estimated the magnetopause distance. The magnetopause distance is the height above the asteroid at which the asteroid's magnetic field would stand off against the solar wind, which is the point that the solar wind pressure and the asteroid's magnetic field pressure balance each other:

$$D = R_p\left(\frac{f^2B^2}{2\mu_0 m_H n\, V^2}\right)^{\frac{1}{6}}$$

where R_p is the radius of the planetesimal (m), m_{H} is the mass of a hydrogen ion (kg), $n = 2$ cm^{-3} is the density of the solar wind at the asteroid belt, $V = 400$ km s^{-1} is the solar wind velocity and $f = 2$ is a geometric factor[54]. B is the field strength on the magnetic equator on the surface (T). For a magnetic dipole, the surface field strength is:

$$B = \frac{\mu_0}{2\pi}\frac{m}{R_m^3},$$

where R_m is the distance from the dipole centre (m). This equation approximates the body's magnetic field as a dipole centred in the body. This approximation is most valid for strong magnetic moments and magnetopause distances that are far from the surface of the body. The magnetopause distances we calculated with this method agree with magnetopauses numerically calculated in more complex hybrid simulations of asteroid magnetospheres in the solar wind[55,56]. However, the concept of a clear magnetopause derived from the pressure balance between the solar wind and the magnetic pressure of an asteroid is not likely to be the case for an asteroid with non-uniform magnetization. An asteroid with a small effective dipole moment generated by groups of smaller, randomly oriented dipoles would have a complicated magnetic field behaviour at close distances that is unknowable a priori. In this case, we assumed that B would be dominated by the dipole that is closest. Thus, we plotted the magnetopause distance assuming that R_m is the same as the length scale of magnetization. To account for impact disruption, we assumed a layer of unmagnetized material nearest the asteroid's surface, and add that thickness to R_m.

Simulation assumptions and parameter uncertainties

Figure 2 applies to planetesimals that formed in the outer Solar System where the nebula dissipated. We chose this time to be 4.8 Myr (ref. [9]). If the nebula dissipated sooner, then the range of formation times that could lead to large-scale magnetization would be narrower. Alternatively, a planetesimal is more likely to retain a CRM if the nebula dissipated later. Our thermal models also assumed that the planetesimals contain 40 vol% water ice. A lower water-to-rock ratio or higher concentration of ^{26}Al in the rock fraction would lead to faster heating and a narrower range of formation times that could result in large-scale magnetization. If heating is sufficiently higher than our nominal scenario, large-scale magnetism dominated by pyrrhotite is not possible because a planetesimal would always exceed pyrrhotite's unblocking temperature. Extended Data Figs. 1 and 2 illustrate the effects of quicker nebular dissipation and a lower water-to-rock ratio, respectively. A 10 vol% water-ice planetesimal would probably not have enough water to undergo complete aqueous alteration, and low water content is not likely in the outer solar system. Furthermore, even if it did occur, magnetite and pyrrhotite may not form, as haematite and tochilinite could be the preferred minerals. Future combined geochemical and thermophysical investigation could reveal which alteration environments produce pyrrhotite and magnetite assemblages that match those within CM and CV chondrites. Regardless, our results illustrate that, thermally, models incorporating greater water ice, or lower heating from a reduced ^{26}Al abundance, are more favourable for large-scale magnetization.

Our thermal model results are largely independent of planetesimal size for radii greater than ~50 km. For smaller planetesimals, the amount of volumetric radiogenic heat generated versus heat lost radiating from the surface becomes an important factor. However, the thermal models are only accurate for diameters greater than approximately

50 km; below this diameter, the assumption of instantaneous migration of liquid water to the surface is not likely to be valid due to low gravity. The models are computed accurately under the assumption that the body separates into a rocky mantle and an overlying water layer. From a thermal evolution standpoint, these models are upper bounds on the max temperature achieved.

The process of aqueous alteration occurs when water ice melts at ~273 K. This assumes that the ice fraction is pure water ice. In our thermal models, the separation of water from rock occurs instantaneously. This assumption is valid if the timescale of water transport is much shorter than the timescale of the thermal evolution[46,48]. This assumption corresponds to bodies with permeabilities greater than ~10^{-14} m^2. The permeability of a planetesimal at early times is difficult to determine. Estimates[24,27] based on geodynamical arguments and/or measurements of meteorites and terrestrial analogues range widely from ~10^{-19} to 10^{-11} m^2. Measurements of permeability in meteorite samples tend to favour low permeability values[24,57]; however, geodynamical models of aqueous alteration often assume high permeability[27,58]. These values need not be in complete agreement. Although the permeability of a meteorite hand sample is low, the overall effective permeability of a planetesimal could be much greater due to large fractures and fluid conduits[37] or because the material has not yet been lithified[21]. If the effective permeability is high, then fluid could flow quickly from the planetesimal's interior to its surface in thousands of years (that is, exhalation flow)[59].

The rate of fluid flow in planetesimals could have controlled the rate of mineral alteration[21]. In this case, the greater the permeability of the planetesimal, the greater the length scale of magnetization. Quick exhalation flow could produce large-scale uniform magnetization of potentially the entire planetesimal body. Per contra, fast exhalation flow might not allow enough time for chemical reactions to occur[59]. Multiple-pass fluid flow (for example, pore-fluid convection) may be required to produce the degree of aqueous alteration seen in CM chondrites[60]. Near the surface of a planetesimal, fluid flow could be dominated by convection[27]. The thermal gradient near the surface would cause warm water to rise while cold water descends. Under this regime, we would expect the magnetization length scale to be approximately the convection length scale. Modelling of pore-fluid convection indicates scales of ~10 km.

Lastly, our modelling assumes that planetesimals instantaneously accreted unaltered material (that is, no alteration during accretion) and that no disruption occurred to the planetesimal during its thermal evolution. Although C-type asteroids could have accreted material that was already aqueously altered to begin with[14], this assumption would not alter our conclusions provided additional alteration could take place. The assumption of instantaneous accretion is acceptable because planetesimals probably formed quickly relative to the timescale of radiogenic heating[61]. Instabilities in the protoplanetary disk could bring together bodies on the order of tens to hundreds of kilometres over thousands of years[51]. Indeed, the theory of planet formation by pebble accretion requires a large reservoir of planetesimals of this size that could subsequently grow into protoplanets by continued aggregation of dust and pebbles. Nevertheless, protracted accretion of a planetesimal may have occurred[62]. And if we were to model this, then we would probably find that the planetesimal formation timing and resulting plausible magnetized volumes would be different, but we do not expect that protracted accretion would nullify our hypothesis that C-type asteroids could retain large-scale magnetization.

Extended Data Fig. 3 illustrates the expected magnetization scale as a function of all the parameters (using a random sample of 50,000 models over the parameter space). These expected magnetization scales are valid for a magnetite-like magnetic carrier and our nominal alteration model, exhalation alteration. A planetesimal with a given set of model parameters matches to one magnetization scale value. The mean magnetization scale we report in Extended Data Fig. 3 is the average value of the magnetization scales for all planetesimal models that fall within a given parameter bin. For example, in the bottom left 2D plot where the axes are accretion time and planetesimal radius, the magnetization scale plotted in the bin located at 3 Myr accretion time and 200 km radius is the mean of a set of random models that all have a 3 Myr accretion time and 200 km radius, but random chosen values for the remaining parameters. The correlation between magnetization scale and planetesimal radii is present mostly because larger planetesimals can have greater magnetization scales simply because they are larger, which skews the average higher. Similarly, the weak decrease in magnetization scale with increasing ice content is due to planetesimals with higher ice content having a smaller radius of silicates after water has separated from the silicates. In general, higher ice contents are thermally more favourable for CRM acquisition, as Extended Data Fig. 2 demonstrates. Overall, we found that a large range of model parameters could produce large-scale uniform magnetization.

Alternative origins of magnetization in planetesimals

Parts of a planetesimal that undergo aqueous alteration could acquire magnetization from either an endogenous or exogenous magnetic field. An endogenous field origin requires that the planetesimal once hosted a dynamo, presumably in a metallic core that was vigorously convecting due to rapid cooling. Therefore, a planetesimal can only host a dynamo if it heated up enough to melt metal and form a liquid core. Chondrites are undifferentiated material; however, they may originate from the outermost shells of parent bodies that were internally differentiated. That is, some chondritic material may remain relatively cold near the surface of a differentiated body[63,64] but experience an endogenous magnetic field from a core dynamo in the hot interior[65]. In other words, steep thermal gradients in the outermost layers of a parent body could keep the exterior cool even if the interior is relatively hot.

The formation of a metallic core could occur as early as a few million years after CAIs for bodies that formed early in the history of the Solar System with scant water ice[63]. However, studies of asteroid dynamos suggest that the onset of a magnetic field would not occur until ~5 Myr after CAIs or later[63,65] because the core needs to start cooling to kickstart a dynamo. Radiogenic dating of carbonate minerals associated with aqueous alteration in CM chondrites places their formation time between ~2.4 and 4 Myr after CAIs[15–18,66]. On the basis of the alteration sequences proposed for CM chondrites, these minerals probably formed contemporaneously with pyrrhotite and magnetite[2,67]. Thus, it is unlikely that an endogenous magnetic field from a core dynamo magnetized the CM chondrites if the model-predicted dynamo timing and the ages of the CM magnetized minerals are correct. Furthermore, the initial abundance of ^{26}Al for the CM and CV chondrites may have been too low to produce enough radiogenic heat to form an iron core[68,69].

A spacecraft detection of a magnetosphere around Pallas, for example, would add evidence to the hypothesis that Pallas has a bulk composition similar to aqueously altered carbonaceous chondrites. Although Pallas probably does not have a metallic core[38], complementary spacecraft measurements that could definitively dismiss the presence of a metallic core would also rule out a dynamo origin for magnetization. Measurements of the density of the near-surface material, compared with the bulk density and (if available) the moment of inertia, would help determine the extent of internal differentiation. Knowledge of the internal differentiation state could constrain whether a metallic core could exist to host a dynamo source[65]. Moreover, the magnetization could not be confused with accretional-detrital-remanent magnetization[70]. Accretional-detrital-remanent magnetization is produced by magnetized grains aligning themselves during the process of accretion in the solar nebular field. However, this magnetization process would not produce uniform magnetization above the metre scale[70,71], and thus only a magnetometer landed on the surface of an asteroid could detect accretional-detrital-remanent magnetization. Thus, observations of large-scale magnetization on Pallas combined with the absence of a metallic core would uniquely confirm that it formed before the solar nebula dissipated.

In principle, a strong solar wind—as opposed to the solar nebular field—could magnetize parts of planetesimals. Although the early solar wind was stronger than the solar wind today, it was probably still ~10–100 times too weak to magnetize chondritic material[52]. Nevertheless, one recent study[72] suggested that the early solar wind could magnetize planetesimals because young planetesimals would behave more like comets and have conductive outer shells that could amplify the magnetizing field by a factor of ~10 near the surface. In this scenario, CM chondrites could originate from the magnetized outer shell of a planetesimal. Whether magnetization by the solar wind could produce a planetesimal with a magnetized shell remains controversial[52].

Past spacecraft observations

So far only one spacecraft with a magnetometer has visited a C-type asteroid. The MASCOT lander aboard JAXA's Hayabusa2 mission made magnetic field measurements on the surface of the C-type, rubble-pile asteroid (162173) Ryugu[73]. However, the MASCOT lander did not detect a magnetic field intrinsic to Ryugu[73]. This means that if Ryugu has magnetization, it must be at a scale less than 1 cm (ref. [73]). This result does not preclude the possibility of magnetized C-type asteroids. First, Ryugu is a rubble pile, so strong uniform magnetization is not possible as any magnetized pebbles or boulders would have scrambled orientations. Furthermore, Ryugu's composition may not match that of aqueously altered chondrites, and thus would not be applicable to this study. However, if samples from Ryugu do match CM chondrites, for example, and do not have any detectable magnetization or evidence that magnetization could have been erased from impacts, then this would suggest that magnetization of CM chondrites is not a ubiquitous process occurring throughout the entire body of an original CM chondrite parent body. Preliminary publications suggest Ryugu is more like CI chondrites[74], which have different magnetic mineralogy than CM chondrites[75].

Although NASA's Dawn spacecraft did not have a magnetometer, Dawn did visit the largest C-type asteroid, 1 Ceres. Using observations from the Gamma Ray and Neutron Detector, one can place an upper limit on Ceres' magnetic field by analysing the deflection of charged particles[76]. Although the Gamma Ray and Neutron Detector made transient detections of deflected particles, it did not observe a signal consistent with a bow shock from a strong dipolar field in the solar wind[76]. According to this argument, Ceres cannot have a magnetic moment greater than ~10^{16} A m^2 or so[76], corresponding to a bulk magnetization of $\leq 10^{-5}$ A m^2 kg^{-1} that is at or below the weakest value considered in Fig. 5. The current detection limit does not rule out large-scale uniform magnetization, so we cannot exclude the possibility that Ceres has a detectable CRM from the solar nebular field. For this reason, future spacecraft magnetometry investigation at Ceres could have immense value because the measurement of an endogenous magnetic field would reveal the extent of Ceres' internal aqueous evolution, which is a priority goal for future Ceres exploration[77].

Data availability

The planetesimal thermal evolution computational model results that support the findings of this study and were used to make the plots are publicly available via the Open Science Framework[78]. Source data are provided with this paper.

Code availability

No custom code or algorithm was developed as part of this work, apart from simple routines written in the MATLAB language that were used to plot simulation data or analytical functions described in the Methods. These routines are available from the corresponding author upon reasonable request. The simulation data were produced using code from a previously published study[48].

References

1. Cournede, C. et al. An early solar system magnetic field recorded in CM chondrites. *Earth Planet. Sci. Lett.* **410**, 62–74 (2015).
2. Fu, R. R. et al. The fine-scale magnetic history of the Allende meteorite: implications for the structure of the solar nebula. *AGU Adv.* **2**, e2021AV000486 (2021).
3. Carporzen, L. et al. Magnetic evidence for a partially differentiated carbonaceous chondrite parent body. *Proc. Natl Acad. Sci. USA* **108**, 6386–6389 (2011).
4. Rubin, A. E., Trigo-Rodríguez, J. M., Huber, H. & Wasson, J. T. Progressive aqueous alteration of CM carbonaceous chondrites. *Geochim. Cosmochim. Acta* **71**, 2361–2382 (2007).
5. MacPherson, G. J. & Krot, A. N. The formation of Ca-, Fe-rich silicates in reduced and oxidized CV chondrites: the roles of impact-modified porosity and permeability, and heterogeneous distribution of water ices. *Meteorit. Planet. Sci.* **49**, 1250–1270 (2014).
6. Stacey, F. D. & Banerjee, S. K. in *The Physical Principles of Rock Magnetism* Vol. 5 (eds Stacey, F. D. & Banerjee, S. K.) 128–135 (Elsevier, 1974); https://doi.org/10.1016/b978-0-444-41084-9.50013-8
7. Stacy, F. D. Paleomagnetism of meteorites. *Annu. Rev. Earth Planet. Sci.* **4**, 147–157 (1976).
8. Pick, T. & Tauxe, L. Chemical remanent magnetization in synthetic magnetite. *J. Geophys. Res. Solid Earth* **96**, 9925–9936 (1991).
9. Weiss, B. P., Bai, X.-N. & Fu, R. R. History of the solar nebula from meteorite paleomagnetism. *Sci. Adv.* **7**, eaba5967 (2021).
10. Borlina, C. S. et al. Paleomagnetic evidence for a disk substructure in the early solar system. *Sci. Adv.* **7**, eabj6928 (2021).
11. Lowrie, W. Identification of ferromagnetic minerals in a rock by coercivity and unblocking temperature properties. *Geophys. Res. Lett.* **17**, 159–162 (1990).
12. Dunlop, D. J., Özdemir, Ö., Clark, D. A. & Schmidt, P. W. Time–temperature relations for the remagnetization of pyrrhotite (Fe_7S_8) and their use in estimating paleotemperatures. *Earth Planet. Sci. Lett.* **176**, 107–116 (2000).
13. Ciesla, F. J., Davison, T. M., Collins, G. S. & O'Brien, D. P. Thermal consequences of impacts in the early solar system. *Meteorit. Planet. Sci.* **48**, 2559–2576 (2013).
14. Desch, S. J., Kalyaan, A. & Alexander, C. M. O. The effect of Jupiter's formation on the distribution of refractory elements and inclusions in meteorites. *Astrophys. J. Suppl. Ser.* **238**, 11 (2018).
15. de Leuw, S., Rubin, A. E., Schmitt, A. K. & Wasson, J. T. ^{53}Mn–^{53}Cr systematics of carbonates in CM chondrites: implications for the timing and duration of aqueous alteration. *Geochim. Cosmochim. Acta* **73**, 7433–7442 (2009).
16. Jilly, C. E. et al. 53Mn-53Cr dating of aqueously formed carbonates in the CM2 lithology of the Sutter's Mill carbonaceous chondrite. *Meteorit. Planet. Sci.* **49**, 2104–2117 (2014).
17. Lee, M. R. et al. Extended chronologies of aqueous alteration in the CM2 carbonaceous chondrites: evidence from carbonates in Queen Alexandra Range 93005. *Geochim. Cosmochim. Acta* **92**, 148–169 (2012).
18. Sugiura, N. & Fujiya, W. Correlated accretion ages and ε^{54}Cr of meteorite parent bodies and the evolution of the solar nebula. *Meteorit. Planet. Sci.* **49**, 772–787 (2014).
19. Verdier-Paoletti, M. J. et al. Testing the genetic relationship between fluid alteration and brecciation in CM chondrites. *Meteorit. Planet. Sci.* **54**, 1692–1709 (2019).
20. Marrocchi, Y., Bekaert, D. V. & Piani, L. Origin and abundance of water in carbonaceous asteroids. *Earth Planet. Sci. Lett.* **482**, 23–32 (2018).
21. Young, E. D., Ash, R. D., Philip, E. & Douglas, R. Fluid flow in chondritic parent bodies: deciphering the compositions of planetesimals. *Science* **286**, 1331–1335 (1999).

22. Scheinberg, A., Fu, R. R., Elkins-Tanton, L. T., Weiss, B. P. & Stanley, S. in *Planetesimals: Early Differentiation and Consequences for Planets* (eds Weiss, B. P. & Elkins-Tanton, L. T.) 180–203 (Cambridge Univ. Press, 2017); https://doi.org/10.1017/9781316339794.009
23. Scheinberg A., Fu R. R., Elkins-Tanton L. T., and Weiss B. P. in Asteroids IV (eds P. Michel et al.) 533–552 (Univ. of Arizona, 2015); https://doi.org/10.2458/azu_uapress_9780816532131-ch028
24. Bland, P. A. et al. Why aqueous alteration in asteroids was isochemical: high porosity ≠ high permeability. *Earth Planet. Sci. Lett.* **287**, 559–568 (2009).
25. Bland, P. A. & Travis, B. J. Giant convecting mud balls of the early solar system. *Sci. Adv.* **3**, e1602514 (2021).
26. Travis, B. J., Bland, P. A., Feldman, W. C. & Sykes, M. V. Hydrothermal dynamics in a CM-based model of Ceres. *Meteorit. Planet. Sci.* **53**, 2008–2032 (2018).
27. Young, E. D., Zhang, K. K. & Schubert, G. Conditions for pore water convection within carbonaceous chondrite parent bodies – implications for planetesimal size and heat production. *Earth Planet. Sci. Lett.* **213**, 249–259 (2003).
28. Ganino, C. & Libourel, G. Reduced and unstratified crust in CV chondrite parent body. *Nat. Commun.* **8**, 261 (2017).
29. King, A. J., Schofield, P. F. & Russell, S. S. Thermal alteration of CM carbonaceous chondrites: mineralogical changes and metamorphic temperatures. *Geochim. Cosmochim. Acta* **298**, 167–190 (2021).
30. King, A. J. et al. The alteration history of the Jbilet Winselwan CM carbonaceous chondrite: an analog for C-type asteroid sample return. *Meteorit. Planet. Sci.* **54**, 521–543 (2019).
31. Tonui, E. et al. Petrographic, chemical and spectroscopic evidence for thermal metamorphism in carbonaceous chondrites I: CI and CM chondrites. *Geochim. Cosmochim. Acta* **126**, 284–306 (2014).
32. Nakamura, T. Post-hydration thermal metamorphism of carbonaceous chondrites. *J. Mineral. Petrol. Sci.* **100**, 260–272 (2005).
33. Neveu, M., Desch, S. J. & Castillo-Rogez, J. C. Core cracking and hydrothermal circulation can profoundly affect Ceres' geophysical evolution. *J. Geophys. Res. Planets* **120**, 123–154 (2015).
34. Ganino, C. & Libourel, G. Fumarolic-like activity on carbonaceous chondrite parent body. *Sci. Adv.* **6**, eabb1166 (2020).
35. Jamieson, J. W. et al. Sulfide geochronology along the Endeavour segment of the Juan de Fuca Ridge. *Geochem., Geophys. Geosystems* **14**, 2084–2099 (2013).
36. Fujii, M., Sato, H., Togawa, E., Shimada, K. & Ishibashi, J. Seafloor hydrothermal alteration affecting magnetic properties of abyssal basaltic rocks: insights from back-arc lavas of the Okinawa Trough. *Earth, Planets Sp.* **70**, 196 (2018).
37. Kaplan, H. H. et al. Bright carbonate veins on asteroid (101955) Bennu: implications for aqueous alteration history. *Science* **370**, eabc3557 (2020).
38. Marsset, M. et al. The violent collisional history of aqueously evolved (2) Pallas. *Nat. Astron*. https://doi.org/10.1038/s41550-019-1007-5 (2020).
39. Schmidt, B. E. & Castillo-Rogez, J. C. Water, heat, bombardment: the evolution and current state of (2) Pallas. *Icarus* **218**, 478–488 (2012).
40. McSween, H. Y. et al. Composition of the Rheasilvia basin, a window into Vesta's interior. *J. Geophys. Res. Planets* **118**, 335–346 (2013).
41. Richardson, J. E. & Abramov, O. Modeling the formation of the lunar upper megaregolith layer. *Planet. Sci. J.* **1**, 2 (2020).
42. Larson, H. P., Feierberg, M. A. & Lebofsky, L. A. The composition of asteroid 2 Pallas and its relation to primitive meteorites. *Icarus* **56**, 398–408 (1983).
43. Macke, R. J., Consolmagno, G. J. & Britt, D. T. Density, porosity, and magnetic susceptibility of carbonaceous chondrites. *Meteorit. Planet. Sci.* **46**, 1842–1862 (2011).
44. Park, R. S. et al. A partially differentiated interior for (1) Ceres deduced from its gravity field and shape. *Nature* **537**, 515–517 (2016).
45. Castillo-Rogez, J. C. & Schmidt, B. E. Geophysical evolution of the Themis family parent body. *Geophys. Res. Lett.* **37**, L10202 (2010).
46. Castillo-Rogez, J. C. & McCord, T. B. Ceres' evolution and present state constrained by shape data. *Icarus* **205**, 443–459 (2010).
47. Castillo-Rogez, J. et al. ^{26}Al decay: heat production and a revised age for Iapetus. *Icarus* **204**, 658–662 (2009).
48. Castillo-Rogez, J. C. et al. Iapetus' geophysics: rotation rate, shape, and equatorial ridge. *Icarus* **190**, 179–202 (2007).
49. Boss, A. P. Evolution of the solar nebula. II. Thermal structure during nebula formation. *Astrophys. J.* **417**, 351 (1993).
50. Wardle, M. Magnetic fields in protoplanetary disks. *Astrophys. Space Sci.* **311**, 35–45 (2007).
51. Johansen, A. & Lambrechts, M. Forming planets via pebble accretion. *Annu. Rev. Earth Planet. Sci.* **45**, 359–387 (2017).
52. Oran, R., Weiss, B. P. & Cohen, O. Were chondrites magnetized by the early solar wind? *Earth Planet. Sci. Lett.* **492**, 222–231 (2018).
53. Cochrane, C. J. et al. Single- and multi-pass magnetometric subsurface ocean detection and characterization in icy worlds using principal component analysis (PCA): application to Triton. *Earth Space Sci.* **9**, e2021EA002034 (2022).
54. Oran, R. et al. Maximum energies of trapped particles around magnetized planets and small bodies. *Geophys. Res. Lett.* **49**, e2021GL097014 (2022).
55. Blanco-Cano, X. & Omidi, N. Hybrid simulations of solar wind interaction with magnetized asteroids: Comparison with Galileo observations near Gaspra and Ida. *J. Geophys. Res. Space Phys.* **108**, 1216 (2003).
56. Fatemi, S., Poppe, A. R., Delory, G. T. & Farrell, W. M. AMITIS: a 3D GPU-based hybrid-PIC model for space and plasma physics. *J. Phys. Conf. Ser.* **837**, 012017 (2017).
57. Corrigan, C. M. et al. The porosity and permeability of chondritic meteorites and interplanetary dust particles. *Meteorit. Planet. Sci.* **32**, 509–515 (1997).
58. Travis, B. J. & Schubert, G. Hydrothermal convection in carbonaceous chondrite parent bodies. *Earth Planet. Sci. Lett.* **240**, 234–250 (2005).
59. Hutchison, R., Pillinger, C., Turner, G., Russell, S. & Young, E. D. The hydrology of carbonaceous chondrite parent bodies and the evolution of planet progenitors. *Phil. Trans. R. Soc. Lond. A* **359**, 2095–2110 (2001).
60. Grimm, R. E. & Mcsween, H. Y. Water and the thermal evolution of carbonaceous chondrite parent bodies. *Icarus* **82**, 244–280 (1989).
61. Morbidelli, A., Bottke, W. F., Nesvorný, D. & Levison, H. F. Asteroids were born big. *Icarus* **204**, 558–573 (2009).
62. Maurel, C. et al. Meteorite evidence for partial differentiation and protracted accretion of planetesimals. *Sci. Adv.* **6**, eaba1303 (2020).
63. Elkins-Tanton, L. T., Weiss, B. P. & Zuber, M. T. Chondrites as samples of differentiated planetesimals. *Earth Planet. Sci. Lett.* **305**, 1–10 (2011).
64. Fu, R. R. & Elkins-Tanton, L. T. The fate of magmas in planetesimals and the retention of primitive chondritic crusts. *Earth Planet. Sci. Lett.* **390**, 128–137 (2014).

65. Bryson, J. F. J., Neufeld, J. A. & Nimmo, F. Constraints on asteroid magnetic field evolution and the radii of meteorite parent bodies from thermal modelling. *Earth Planet. Sci. Lett.* **521**, 68–78 (2019).
66. Fujiya, W., Sugiura, N., Sano, Y. & Hiyagon, H. Mn–Cr ages of dolomites in CI chondrites and the Tagish Lake ungrouped carbonaceous chondrite. *Earth Planet. Sci. Lett.* **362**, 130–142 (2013).
67. Suttle, M. D., King, A. J., Schofield, P. F., Bates, H. & Russell, S. S. The aqueous alteration of CM chondrites, a review. *Geochim. Cosmochim. Acta* **299**, 219–256 (2021).
68. Fukuda, K. et al. A temporal shift of chondrule generation from the inner to outer Solar System inferred from oxygen isotopes and Al-Mg chronology of chondrules from primitive CM and CO chondrites. *Geochim. Cosmochim. Acta* **322**, 194–226 (2022).
69. Nagashima, K., Krot, A. N. & Komatsu, M. ^{26}Al–^{26}Mg systematics in chondrules from Kaba and Yamato 980145 CV3 carbonaceous chondrites. *Geochim. Cosmochim. Acta* **201**, 303–319 (2017).
70. Fu, R. R. & Weiss, B. P. Detrital remanent magnetization in the solar nebula. *J. Geophys. Res. Planets* **117**, E02003 (2012).
71. Biersteker, J. B. et al. Implications of Philae magnetometry measurements at comet 67P/Churyumov–Gerasimenko for the nebular field of the outer solar system. *Astrophys. J.* **875**, 39 (2019).
72. O'Brien, T. et al. Arrival and magnetization of carbonaceous chondrites in the asteroid belt before 4562 million years ago. *Commun. Earth Environ.* **1**, 54 (2020).
73. Hercik, D. et al. Magnetic properties of asteroid (162173) Ryugu. *J. Geophys. Res.* **125**, e06035 (2020).
74. Yada, T. et al. Preliminary analysis of the Hayabusa2 samples returned from C-type asteroid Ryugu. *Nat. Astron*.https://doi.org/10.1038/s41550-021-01550-6 (2021).
75. Sridhar, S., Bryson, J. F. J., King, A. J. & Harrison, R. J. Constraints on the ice composition of carbonaceous chondrites from their magnetic mineralogy. *Earth Planet. Sci. Lett.* **576**, 117243 (2021).
76. Villarreal, M. N. *Understanding the Interiors of Vesta and Ceres Through Their Interactions with the Solar Wind* (Univ. California Los Angeles, 2018).
77. Castillo-Rogez, J. et al. Science drivers for the future exploration of Ceres: from solar system evolution to ocean world science. *Planet. Sci. J.* **3**, 64 (2022).
78. Courville, S. Courville_etal_2022_planetesimal_thermal_models. *Open Science Framework* https://doi.org/10.17605/OSF.IO/WAHN2 (2022).
79. Scheinberg, A., Elkins-Tanton, L. T., Schubert, G. & Bercovici, D. Core solidification and dynamo evolution in a mantle-stripped planetesimal. *J. Geophys. Res. Planets* **121**, 2–20 (2016).

Acknowledgements

We thank A. Rubin for fruitful discussions about the alteration of CM chondrites. B.P.W., R.O. and L.T.E.-T. thank the NASA Discovery Program (grant number NNM16AA09C) for support. Part of this work was carried out at the Jet Propulsion Laboratory, California Institute of Technology, under a contract with the National Aeronautics and Space Administration (80NM0018D0004).

Author contributions

S.W.C. and J.G.O. designed the modelling study. S.W.C. performed the model analysis, created the figures and wrote the manuscript. J.C.C.-R. provided the thermal evolution model data. R.O. provided the methodology for the magnetopause calculation. B.P.W. and R.R.F. guided discussion of the magnetization within chondrites. L.T.E.-T. guided discussion of planetesimal formation. All authors provided comments and edits during the drafting of the manuscript.

Competing interests

The authors declare no competing interests.

Additional information

Extended data is available for this paper at https://doi.org/10.1038/s41550-022-01802-z.

Supplementary information The online version contains supplementary material available at https://doi.org/10.1038/s41550-022-01802-z.

Correspondence and requests for materials should be addressed to Samuel W. Courville.

Peer review information *Nature Astronomy* thanks Clara Maurel and the other, anonymous, reviewer(s) for their contribution to the peer review of this work.

Reprints and permissions information is available at www.nature.com/reprints.

https://doi.org/10.1038/s41550-022-01802-z

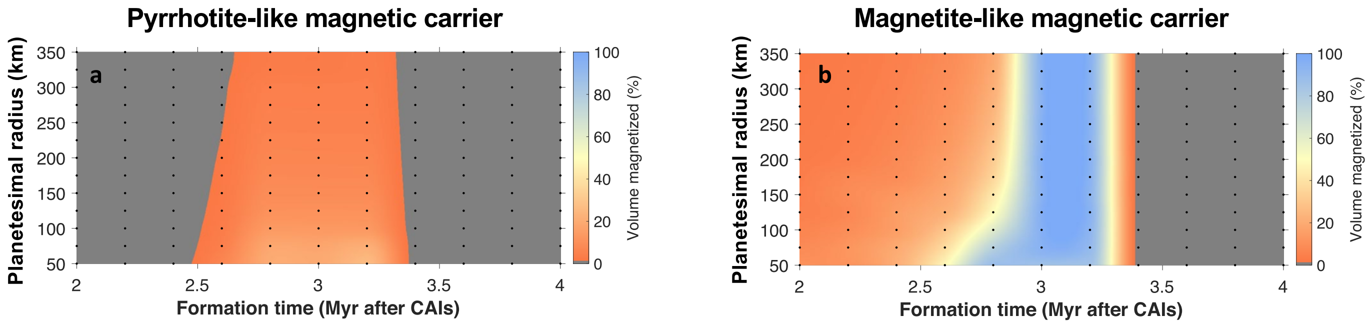

Extended Data Fig. 1 | Magnetization preservation for inner solar system nebula dissipation time. Maximum magnetized volume percent for planetesimals with 40 vol% water ice that formed in the inner solar system where the solar nebula dissipated at 3.9 Myr after CAIs and assuming an unblocking temperature of (a) 550 K and (b) 850 K, which correspond to the magnetic carriers pyrrhotite and magnetite respectively. Quicker nebula dissipation leads to fewer planetesimals that could be magnetized. Compared to the nominal case in Fig. 2, the range of time that can lead to complete magnetization has been greatly reduced if magnetite is the carrier and eliminated if pyrrhotite is the carrier.

 https://doi.org/10.1038/s41550-022-01802-z

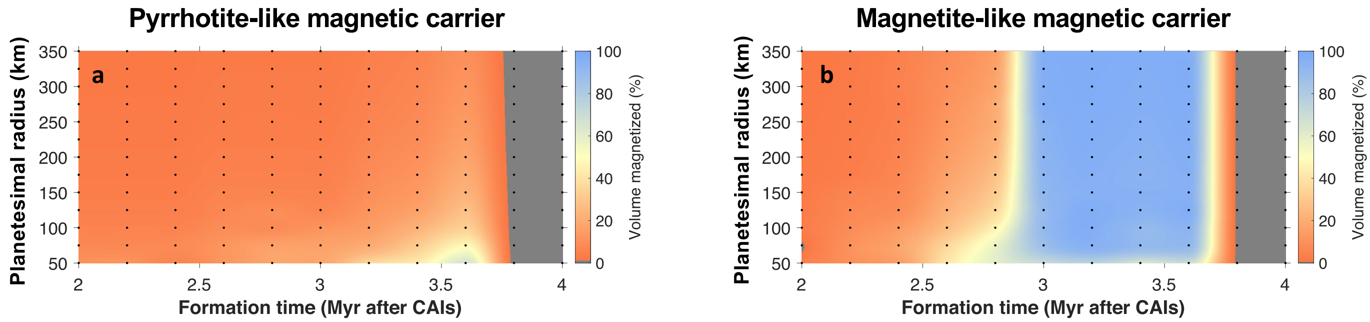

Extended Data Fig. 2 | Magnetization preservation for planetesimals that accreted less water ice. Maximum magnetized volume percent for planetesimals with 10 vol% water ice that formed in the outer solar system where the solar nebula dissipated at 4.8 Myr after CAIs and assuming an unblocking temperature of (a) 550 K and (b) 850 K, which corresponds to the magnetic carrier being pyrrhotite and magnetite respectively. Because there is less water ice, there is more radiogenic heating. More radiogenic heating means it is easier to reach the unblocking temperature(s) and erase magnetization. Compared to the nominal case in Fig. 2, the range in time that allows for complete magnetization assuming magnetite is the magnetic carrier has been narrowed. No times allow complete magnetization assuming pyrrhotite is the carrier.

https://doi.org/10.1038/s41550-022-01802-z

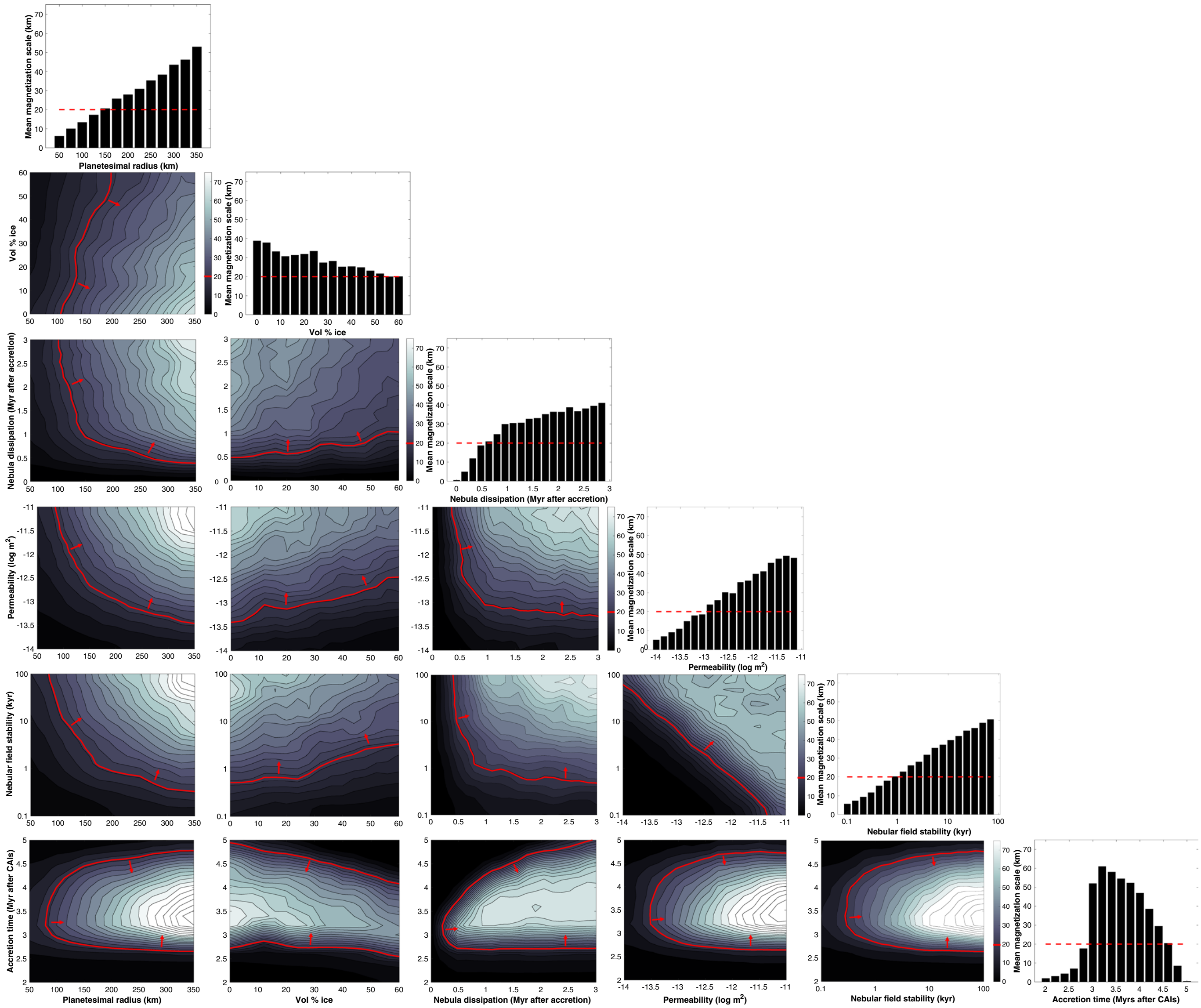

Extended Data Fig. 3 | Mean magnetization scale as a function of the exhalation alteration parameters, assuming a magnetite-like magnetic carrier. The mean magnetization scale is the average of the magnetization scale values for every planetesimal model run within a given bin of parameter values. We generated this plot from 50,000 random samples of the parameter space. The mean magnetization scale for the entire set of models is 30 km.